Dynamics of Davydov solitons

Alwyn C. Scott
Center for Nonlinear Studies, Los Alamos National Laboratory, Los Alamos, New Mexico 87545
(Received 29 October 1981)

After modifying Davydov's original equations for the α-helix soliton to include ten additional dipole-dipole coupling terms and to represent helical symmetry, a numerical study predicts that such solitons should appear under normal physiological conditions. This conclusion is supported by the assignment of a recently measured laser-Raman spectrum of a metabolically active cell to internal vibrations of the soliton. Analytical studies of continuum approximations to the numerical model provide additional insight into the soliton dynamics.

I. INTRODUCTION

A soliton is essentially a one-dimensional object that maintains dynamic integrity by balancing the effects of nonlinearity against those of dispersion,[1] and polymers are real dynamic systems that exhibit both dispersion and nonlinearity. Thus one should not be surprised to find solitons on polymers, and several recent investigations indicate that this may indeed be the case in such diverse structures as β-phase polyvinylidene fluoride $(PVF_2)_x$,[2] polyacetylene (CH_x),[3] and deoxyribonucleic acid (DNA).[4] Closely related are the charge-density-wave solitons found on certain one-dimensional conductors.[5]

Perhaps the earliest suggestion for a "polymer soliton" was made by Davydov[6] in an attempt to solve an outstanding riddle of biochemistry. To understand the background note that (i) biological energy is released in units of about 0.49 eV by hydrolysis of adenosine triphosphate (ATP) to ADP,[7] and (ii) a basic biological resonance is the double-bonded carbon-oxygen (or amide-I bond) which has a quantum energy of 0.205 eV (1650 cm^{-1}) and is found in every peptide group of every protein. The amide-I bond appears of interest, therefore, as a "basket" for storage and transport of biological energy. It has not been seriously so considered because the linewidths of typical amide-I absorption peaks imply a lifetime (due to dipole-dipole coupling between amide-I bonds) of the order of 10^{-12} sec, i.e., much too short for normal biological mechanisms.[8] Davydov's idea is that this lifetime can be markedly increased on an α-helix protein (see Fig. 1) in the following way:

(a) introduction of localized amide-I bond energy induces longitudinal sound waves on the helix;
(b) longitudinal sound acts as a potential well to trap the bond energy and prevent its dispersion.

This interaction can be represented symbolically as

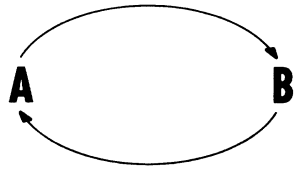

emphasizing that the two effects acting together constitute a *dynamically self-sufficient entity.* From the chemist's perspective it can be described as a *mobile region of conformational change.*

The analytical theory of this soliton has been discussed in a number of papers by Davydov and

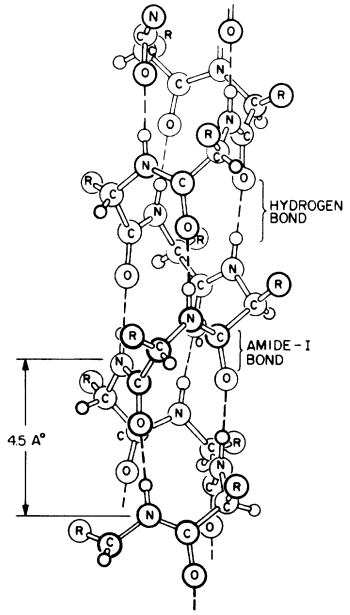

FIG. 1. α helix (redrawn from Ref. 9 with permission of the author).

his co-workers[6] from which it is seen that anharmonicity in the longitudinal hydrogen bonds plays a major role in effecting the mechanisms (a) and (b) described above. In a previous publication it has been shown that, for a given level of total bond energy, there is a threshold level of anharmonicity below which the soliton will not form.[10] An order-of-magnitude analysis indicated that hydrogen-bond anharmonicity in a real α helix is about the right magnitude to support soliton formation. In this paper a more precise test of this question is presented.

It should perhaps be emphasized that there is little doubt about the ability of an α helix to support and conduct solitons. That is not the issue. The question is whether a normal amount of biological energy is sufficient to form a soliton. Since 0.49 eV is released by ATP hydrolysis under normal physiological conditions and a quantum of amide-I bond energy is 0.205 eV, two quanta are taken as a biologically feasible amount of soliton energy. An important parameter in this study, χ_1 is the change in amide-I bond energy (N m) per unit extension (m) of the hydrogen bond. (Throughout this paper the term "hydrogen-bond anharmonicity" is used for χ_1.) Values for χ_1 can be calculated in two entirely different ways.

(i) Find the value of χ_1 for the hydrogen bond in a real α helix. This has not yet been done. But a self-consistent-field (SCF) calculation[11] for a similar bond in a formamide dimer (see Fig. 2) yields the value[12] $\chi_1 = 0.34 \times 10^{-10}$ N.

(ii) Using the best possible numerical model of an α-helix protein and the above-mentioned two quanta of total amide-I bond energy, calculate the value of χ_1 at which solitons form.

Calculation of item (ii) is the main aim of this paper.

I do not wish to suggest that the solitons described here are the only ones to be found in biological systems. Quite the contrary. Indeed, Davydov has described a mechanism similar to that considered here for the transport of electronic charge,[13] and a "topological" soliton on DNA is described.[4] Also Bilz *et al.* have recently discussed biological applications of a soliton that involves the interaction of sound waves with electric polarization.[14] The present mechanism is one of several

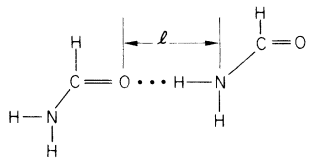

FIG. 2. Formamide dimer ($l = 2.99 \pm 0.12$ Å).

to which biochemists should be giving serious attention.

Section II presents a summary of the various systems of equations that are discussed. These include Davydov's system (*D*) and two approximate systems [the Zakharov system (*Z*) and the nonlinear Schrödinger system (NLS)], which are convenient for certain analytical studies. In addition, a modified Davydov system (MD) has been developed to ensure accuracy in the numerical determination of χ_1. In Sec. III the various physical parameters for MD are discussed and recorded, and results of the threshold computation for χ_1 are presented. Section IV shows how the threshold for soliton formation can be obtained from the NLS equation and the "inverse scattering transform" of soliton theory. In Sec. V a soliton perturbation theory is applied to the *Z* system to clarify certain aspects of the soliton dynamics and structure. Of particular importance is the study of interactions between the soliton and various modes of mechanical vibration. In Sec. VI it is concluded that solitons should be expected to appear in the biological functioning of α-helix protein. This conclusion is followed by a listing of several speculations that have appeared in the literature concerning the possibility of observing α-helix solitons in real experiments. The last item in this list is the most important. It came to my attention after this manuscript had been completed that the laser-Raman spectrum of metabolically active cells in the range below 200 cm^{-1} is precisely explained from previously calculated internal vibrations of the α-helix soliton with no "adjustment of parameters" whatsoever. This observation indicates that Davydov solitons play a functional role in vital processes. Certain auxiliary discussions (the structure of the wave function used in MD, details of the perturbation analysis, and a discussion of the effects of extra dipole-dipole coupling terms) are relegated to appendixes in order not to impede the flow of presentation.

II. EQUATIONS TO BE CONSIDERED

In this section several systems of equations to describe the dynamics of an α helix are displayed and discussed. We begin with the most elaborate system developed by Davydov and his co-workers[15]; this is also

the system that was previously studied numerically in Ref. 10. We shall refer to it as the "Davydov" (D) system:

$$i\hbar\frac{da_{n\alpha}}{dt}=[E_0+W+\chi_1(\beta_{n+1,\alpha}-\beta_{n-1,\alpha})]a_{n\alpha}-J(a_{n+1,\alpha}+a_{n-1,\alpha}) +L(a_{n,\alpha+1}+a_{n,\alpha-1})+\chi_2[(\beta_{n+1,\alpha}-\beta_{n\alpha})a_{n+1,\alpha}+(\beta_{\eta\alpha}-\beta_{n-1,\alpha})a_{n-1,\alpha}] , \tag{2.1a}$$

$$M\frac{d^2\beta_{n\alpha}}{dt^2}-w(\beta_{n+1,\alpha}-2\beta_{n\alpha}+\beta_{n-1,\alpha})=\chi_1(|a_{n+1,\alpha}|^2-|a_{n-1,\alpha}|^2) +\chi_2[a^*_{n\alpha}(a_{n+1,\alpha}-a_{n-1,\alpha})+(a^*_{n+1,\alpha}-a^*_{n-1,\alpha})a_{n\alpha}] , \tag{2.1b}$$

$$W\equiv\tfrac{1}{2}\sum_{n,\alpha}\left[M\left[\frac{d\beta_{n\alpha}}{dt}\right]^2+w(\beta_{n\alpha}-\beta_{n-1,\alpha})^2\right] . \tag{2.1c}$$

To appreciate these "D-equations" in detail, the reader should study them in relation to a chemical diagram of the α helix such as Fig. 1. In addition to the basic helix with the valence-bonded sequence:

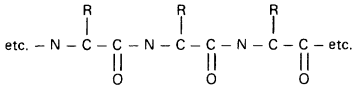

(where the R's are residues that specify the detailed character of the protein), three almost longitudinal "spines" can be seen with the sequence:

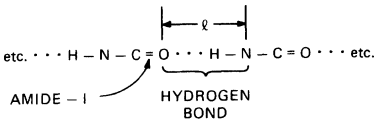

The hydrogen bonds of these three spines hold the protein in its helical form. They have a length[16] $l=2.9\pm0.1$ Å which is about equal to that of the formamide dimer shown in Fig. 2.

In the D equations, the index n specifies a particular unit cell counting longitudinally along the helix, while α specifies a particular spine and takes the values 1, 2, or 3. Thus the pair (n,α) picks out a single peptide unit and amide-I bond. The terms in (2.1) have the following significance: $a_{n\alpha}$ is the probability amplitude for occupation of the amide-I bond located at (n,α); E_0 is the quantum energy of an amide-I vibration; $\beta_{n\alpha}$ is the longitudinal displacement of the peptide unit located at (n,α); M is one-third of the molecular weight of a unit cell; w is the linear restoring force of a hydrogen bond; W is the total energy of the longitudinal sound; J is the dipole-dipole coupling energy between a particular amide-I bond and those ahead and behind along the same spine; and L is the dipole-dipole coupling between a particular amide-I bond and those on adjacent spines in the same unit cell.

Two parameters in the D equations remain to be discussed: χ_1 and χ_2. If both are zero, (2.1a) describes dispersion of amide-I bond energy that is uncoupled from the propagation of longitudinal sound which is governed by (2.1b). As is explained, in Ref. 17, these terms relate the change in energy of an amide-I bond to longitudinal extension of the helix. Thus in (2.1a) the term

$$\chi_1(\beta_{n+1,\alpha}-\beta_{n\alpha})$$

gives the change in energy of the amide-I bond at (n,α) caused by stretching of the helix between $n+1$ and n; and

$$\chi_2(\beta_{n+1,\alpha}-\beta_{n,\alpha})a_{n+1,\alpha}$$

gives the change in longitudinal coupling between (n,α) and $(n+1,\alpha)$ (i.e., change in the J term) caused by stretching of the helix between $n+1$ and n. These terms are derived from interaction contributions to the total Hamiltonian of the form

$$H^{(1)}_{\rm int}=\chi_1\sum_{n\alpha}a^*_{n\alpha}a_{n\alpha}[(\beta_{n+1,\alpha}-\beta_{n\alpha})+(\beta_{n\alpha}-\beta_{n-1,\alpha})] , \tag{2.2}$$

$$H^{(2)}_{\rm int}=\chi_2\sum_{n\alpha}(\beta_{n\alpha}-\beta_{n-1,\alpha})(a^*_{n\alpha}a_{n-1\alpha}+a^*_{n-1,\alpha}a_{n\alpha}) , \tag{2.3}$$

thus corresponding terms are introduced into (2.16b).

The interaction parameter χ_2 is easily computed because the longitudinal dipole-dipole coupling energy (J terms) is inversely proportional to the cube of the longitudinal distance (d) between adjacent peptide units. Thus[18]

$$\text{Total longitudinal coupling} = -\frac{Jd^3}{(d+\Delta\beta)^3}$$

$$\doteq -J+\frac{3J}{d}\Delta\beta$$

and therefore

$$\chi_2=\frac{3J}{d} . \tag{2.4a}$$

For $J=7.8\ \text{cm}^{-1}$ (Ref. 19) and $d=4.5$ Å (Ref. 16)

$$\chi_2=10^{-12}\ \text{N} . \tag{2.4b}$$

As was noted in Sec. I, the interaction parameter χ_1 has been calculated for the hydrogen bond of a similar molecule[12] shown in Fig. 2 as

$$\chi_1=34\times10^{-12}\ \text{N} . \tag{2.5}$$

Thus the terms involving χ_2 are of minor importance in the dynamics of system D. The strategy in this paper is to keep χ_2 at the value given in (2.4a) and determine the threshold level of χ_1 at which solitons form. This threshold value for χ_1 will then be compared with the value given in (2.5).

Before leaving D, we note that a film of soliton formation on this system has been prepared by Eilbeck under the assumption $\chi_1=\chi_2$.[20] This film gives a dramatic confirmation of the results discussed in Ref. 10: the threshold for soliton formation, robustness of the soliton with respect to noise in the sound system, and bond-energy dispersion below soliton threshold.

Numerical study of D (Refs. 10 and 20) shows that several unit cells are included in a single soliton. Thus it is interesting to consider a distributed approximation to D where the discrete longitudinal index n is interpreted as a continuous space variable x. Then with appropriate normalizations[6,10,15] and defining

$$\rho\propto-\frac{\partial\beta}{\partial x} , \tag{2.6}$$

the D system reduces to

$$iA_t+A_{xx}=-k_1\chi\rho A , \tag{2.7a}$$

$$\rho_{xx}-\frac{1}{\bar{c}^2}\rho_{tt}=k_2\chi(|A|^2)_{xx} . \tag{2.7b}$$

Here $|A|^2$ is the longitudinal density of bond quanta (on all three spines), $\chi\equiv\chi_1+\chi_2$, $\bar{c}$ is the longitudinal sound speed, and k_1 and k_2 are constants that are determined from the energetic parameters of the problem. These equations are called the "Zakharov" (Z) system because they first arose under that name in the context of plasma physics.[21] The Z equations clearly show the nature of the "region of conformational change" described in Sec. I. Localized bond energy ($|A|^2$) acts as a source of longitudinal sound in (2.7b). This sound (ρ) serves as a potential well in (2.7a) to prevent dispersion of bond energy.

Since the solitons of D move slowly with respect to the speed of longitudinal sound,[10] the ρ_{tt} term in (2.7b) is only a small fraction of the ρ_{xx} term. Defining

$$\text{soliton speed} \equiv s\bar{c} \tag{2.8}$$

and introducing the further normalizations: $t=\tau/\bar{c}^2$, $x=\xi/\bar{c}$, $A=\tilde{A}/\bar{c}^2$, and $\rho=\tilde{\rho}/\bar{c}^2$, (2.7) reduces to the nonlinear Schrödinger (NLS) equation

$$i\tilde{A}_\tau+\tilde{A}_{\xi\xi}=-\frac{k_1k_2\chi^2}{(1-s^2)\bar{c}^6}|\tilde{A}|^2\tilde{A} , \tag{2.9}$$

which can be studied using the inverse scattering transform method of soliton theory.[10,22,23] Such calculations are sketched in Sec. IV, but here it is convenient to notice that the critical value of the interaction parameter (χ_c) is proportional to $(\bar{c})^3$, and since sound speed is inversely proportional to the square root of M (the molecular weight of a single repeating unit along the helix), we expect

$$\chi_c\propto M^{-3/2} . \tag{2.10}$$

In pursuing numerical studies of D beyond those reported,[10] it was observed that additional dipole-dipole interaction terms *increase* the critical level of the interaction parameter (χ_{1c}) at which soliton formation occurs. This is a serious error because the aim of the numerical study is to see whether χ_{1c} is greater than the computed value of χ_1 given in (2.5). Thus it was necessary to include enough terms of dipole-dipole interaction so that χ_{1c} is insensitive to the introduction of additional terms. The details of determining how many extra terms are "enough" are discussed in Appendix A, but, briefly stated, it was necessary to add ten additional coupling terms to (2.1a). Furthermore, (2.1) does not represent a true helical structure, but rather "disks" (indexed by n) connected by three "springs" (indexed by α). With both of these changes, (2.1a) takes the modified Davydov (MD) form

$$i\hbar\frac{da_{n\alpha}}{dt}=[E_0+0+\chi_1(\beta_{n+1,\alpha}-\beta_{n-1,\alpha})]a_{n\alpha}-J(a_{n+1,\alpha}+a_{n-1,\alpha})$$
$$+\chi_2[a_{n+1,\alpha}(\beta_{n+1,\alpha}-\beta_{n\alpha})+a_{n-1,\alpha}(\beta_{n\alpha}-\beta_{n-1,\alpha})]$$
$$+LF_L+NF_N+PF_P+QF_Q+RF_R+SF_S+TF_T+UF_U+VF_V+XF_X+ZF_Z\ . \tag{2.11}$$

There were no changes made in (2.1b).

The term "LF_L" in (2.11) differs from the corresponding term in (2.1a) to account for a helical structure. Thus

$$i\hbar\dot{a}_{n\alpha}=L(a_{n,\alpha+1}+a_{n,\alpha-1})+\cdots$$

in (2.1a) is changed to

$$\begin{aligned} i\hbar\dot{a}_{n1}&=L(a_{n2}+a_{n-1,3})+\cdots\ ,\\ i\hbar\dot{a}_{n2}&=L(a_{n3}+a_{n1})+\cdots\ ,\\ i\hbar\dot{a}_{n3}&=L(a_{n2}+a_{n+1,1})+\cdots\ . \end{aligned} \tag{2.12}$$

The terms on the right-hand side of (2.12) are indicated symbolically as LF_L in (2.11). The structures of the ten additional coupling terms in (2.11) are listed in Appendix A.

The "0" that appears in the first line of (2.11) emphasizes one further modification of (2.1a). As derived by Davydov *et al.*,[15] the system D is subject to the constraint

$$\sum_{n\alpha}|a_{n\alpha}|^2=1\ ,$$

which implies that only a single quantum of amide-I bond energy is present in a soliton. However, as was noted in Sec. I, hydrolysis of ATP to ADP under normal physiological conditions releases about 0.49 eV of free energy[7] which is more than twice the amide-I vibrational quantum energy (0.205 eV). Thus it is of interest to consider the possibility that a soliton contains two quanta of amide-I bond energy, or more generally that

$$\sum_{n\alpha}|a_{n\alpha}|^2=N\ . \tag{2.13}$$

A modification of Davydov's fundamental wave function that allows this more general case is described in Appendix B. An effect of this modification is to remove the "W term" from the first line of (2.1a). In the numerical studies, however, no difference was observed in the dynamics of $\beta_{n\alpha}$ and $|a_{n\alpha}|^2$ upon removal of W. This is to be expected since W is approximately constant and contributes only to a phase advance of $a_{n\alpha}$. The whole question is more aesthetic than practical.

III. NUMERICAL OBSERVATIONS OF THRESHOLD

For numerical studies it is convenient to write (2.11) and (2.1b) in the normalized form

$$\frac{dA_{n\alpha}}{d\tau}=\left[\frac{1}{\hbar}\left[\frac{M}{w}\right]^{1/2}\times10^{-21}\right]\{(10^{10}\chi_1)(B_{n+1,\alpha}-B_{n-1,\alpha})A_{n\alpha}+(10^{10}\chi_2)$$
$$\times[B_{n+1,\alpha}A_{n+1,\alpha}-B_{n-1,\alpha}A_{n-1,\alpha}-B_{n\alpha}(A_{n+1,\alpha}-A_{n-1,\alpha})]\}$$
$$+\frac{1}{\hbar}\left[\frac{M}{w}\right]^{1/2}[-J(A_{n+1,\alpha}+A_{n-1,\alpha})+LF_L+\cdots+ZF_Z]\ , \tag{3.1a}$$

$$\frac{d^2B_{n\alpha}}{d\tau^2}-(B_{n+1,\alpha}-2B_{n\alpha}+B_{n-1,\alpha})=\left[\frac{1}{0.1w}\right]\{(10^{10}\chi_1)(|A_{n+1\alpha}|^2-|A_{n-1\alpha}|^2)$$
$$+(10^{10}\chi_2)[A^*_{n\alpha}(A_{n+1,\alpha}-A_{n-1,\alpha})+A_{n\alpha}(A^*_{n+1,\alpha}-A^*_{n-1,\alpha})]\}\ , \tag{3.1b}$$

where

$$a_{n\alpha} \equiv A_{n\alpha} \exp(-iE_0 t/\hbar) , \tag{3.2a}$$

$$\beta_{n\alpha} \equiv B_{n\alpha} \times 10^{-11} , \tag{3.2b}$$

in units of meters,

$$\tau \equiv t\sqrt{w/M} . \tag{3.2c}$$

Thus (3.2a) absorbs the fast phase advance of the amide-I bond amplitude, (3.2b) measures longitudinal displacement in units of 0.1 Å, and (3.2c) measures time in units of $\sqrt{M/w}$ sec.

For the results presented here, M was taken as the average mass of a repeat distance in myosin from rabbit skeletal muscle; thus[24] $M = 114.2\times$ mass of proton. The spring constant for the hydrogen bond displayed in Fig. 2 has been computed by Kuprievich and Kudritskaya[12] as 21 N/m. Considering that the hydrogen bonds in α helix are oriented 22° away from the longitudinal direction, we take

$$w = 19.5 \tag{3.3}$$

in units of N/m, thus

$$\left[\frac{M}{w}\right]^{1/2} = 0.99\times 10^{-13} \tag{3.4}$$

in units of sec.

As was mentioned previously, χ_2 is set at the value given in (2.4b), while χ_1 is left as a variable parameter.

The dipole-dipole interaction terms are given in Table I where J through Q are obtained from Ref. 19 and R through Z are computed as indicated in Ref. 25.

TABLE I. Energies for dipole-dipole interactions.

Term	Energy (cm^{-1})	Energy (computer units)
J	7.8	0.145
L	12.4	0.231
N	3.9	0.073
P	1.8	0.034
Q	1.0	0.019
R	0.64	0.012
S	0.48	0.0089
T	0.39	0.0073
U	0.20	0.0037
V	0.16	0.0030
X	0.12	0.0022
Z	0.091	0.0017

The boundary conditions required $A_{n\alpha}=0$ and $B_{n\alpha}=0$ for $n=-3, -2, -1, n_{\max}+1, n_{\max}+2,$ and $n_{\max}+3$, where $n_{\max}$ is the total number of unit cells considered to be in the molecule. The initial conditions were

$$\begin{aligned} &|A_{01}|^2 = |A_{02}|^2 = 1 , \\ &\text{All other } |A_{n\alpha}|^2 = 0 , \\ &\text{All } B_{n\alpha} = 0 \end{aligned} \tag{3.5}$$

at time $\tau=0$. From a physical point of view, this means that one quantum was introduced into each of the first two amide-I bonds at the initial time. This seems reasonable from a chemical perspective; it also leads to the most natural soliton formation from two quanta.

A typical example of the numerical output is displayed in Fig. 3. Here $n_{\max}=200$, which corresponds to the 1000 Å of a typical myosin molecule in skeletal muscle. On the upper scale, a soliton is seen emerging from the background of bond energy. On the lower scale, sound energy is divided into two components: A which is locked into the motion of the soliton, and B which is induced by the initial conditions and travels at (unit) sound speed.

Computations to determine the threshold level of χ_1 for a soliton to form are plotted in Fig. 4. Here again $n_{\max}=200$ and $\tau=400$. For $\chi_1 \le 0.3\times 10^{-10}$ N the response is essentially that of a linear dispersive system. As $10^{10}\chi_1$ is increased from 0.3 to 0.4 (see Fig. 5) a soliton forms, and as $10^{10}\chi_1$ is increased above 0.6, an immobile conformational change appears at the origin. Thus we find a "window" for soliton formation when χ_1 lies in the range

$$0.35\times 10^{-10} \le \chi_1 \le 0.6\times 10^{-10} \text{ N} . \tag{3.6}$$

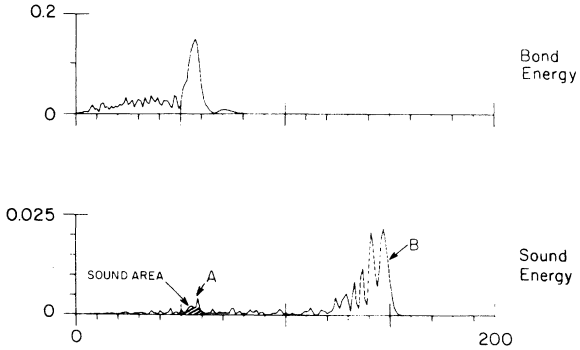

FIG. 3. Bond energy and sound energy.

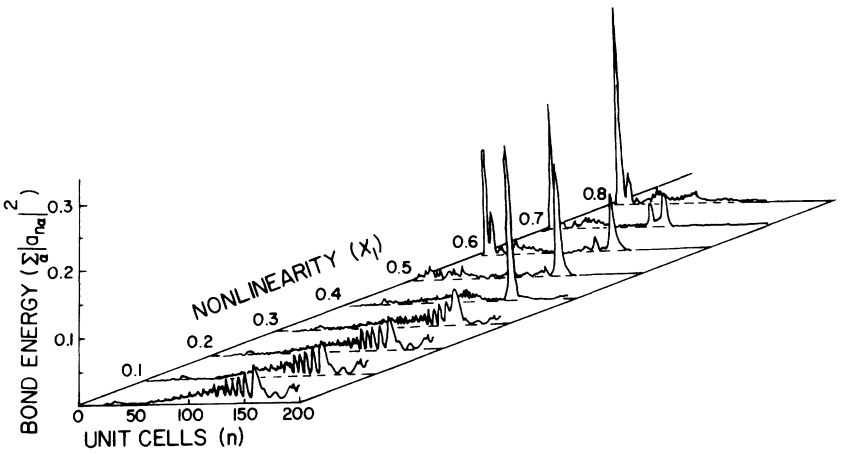

FIG. 4. Threshold calculation at $\tau=400$.

The value of $\chi_1(=0.34\times10^{-10}$ N) computed by Kuprievich and Kudritskaja[12] lies just on the sill of this window.

At $\chi_1=0.4\times10^{-10}$ N the soliton speed is $\frac{3}{8}$ of the sound speed, which, in turn, is $(w/M)^{1/2}$ times the length of a unit cell (4.5 Å) or 4.55×10^3 cm/sec. Thus

$$s\bar{c}=1.7\times10^3 \tag{3.7}$$

in units of cm/sec. It is important to observe that the design of protein mechanisms involving solitons need not rely on happenstance to ensure that the actual level of hydrogen bond anharmonicity (χ_1) lies within the above-mentioned window for soliton formation. Appropriate cross linkages, for example, in the "coiled-coil" configuration of two α helices so often found in motile tissue,[26] provide the option of increasing the effective value of M by a significant factor and thereby, through (2.10), decreasing the critical level of χ_1 for soliton formation.

Next it is interesting to take a closer look at the structure of the soliton. Figure 6 displays some computations on a molecule of 100 unit cells $(n_{\max}=100)$ with initial conditions as in (3.5) and $\chi_1=0.4\times10^{-10}$ N. In addition to the *total* bond energy,

$$|A_{n1}|^2+|A_{n2}|^2+|A_{n3}|^3,$$

that portion located on each of the three spines is plotted versus n for various times τ. While the total energy propagates uniformly as a solitary wave, the individual spine energies are oscillating in amplitude and position with respect to the sum. At $\tau=150-152$ energy is maximum on spine No. 1. From $158-162$, it is maximum on spine No. 2 and from $\tau=164-168$ it is maximum on spine No. 3. At $\tau=170$, spine No. 1 has recovered its status as maximum. This oscillatory behavior has a period of about 20τ or, from (3.2c),

$$\mathscr{P}\doteq2\times10^{-12} \tag{3.8}$$

in units of sec.

Finally in Fig. 7 we consider the dynamics of a molecule over a time scale long enough to observe reflections from the ends. Initial conditions are as in (3.5), $\chi_1=0.4\times10^{-10}$ N and there are 100 unit cells $(n_{\max}=100)$. During the time $0<\tau<270$, a well-developed soliton propagates to the right. During the time $270<\tau<540$ a pulse travels to the left but its solitary-wave character becomes gradually dissipated. For times greater than about 540, the bond energy is distributed over the molecule in an almost completely chaotic manner. Numerical experiments with molecules of different lengths show that soliton dissipation is dominated by interaction with the tail. Thus in general the soliton can be viewed as a "critically damped" oscillator

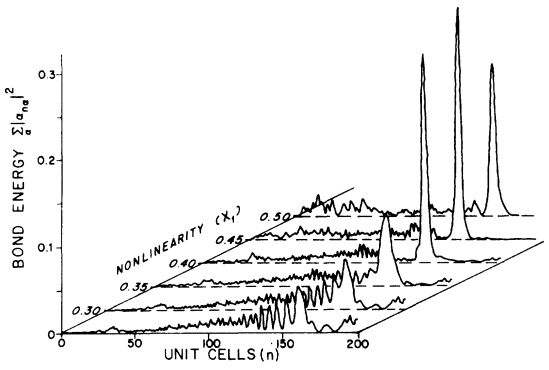

FIG. 5. Expanded threshold calculation at $\tau=400$.

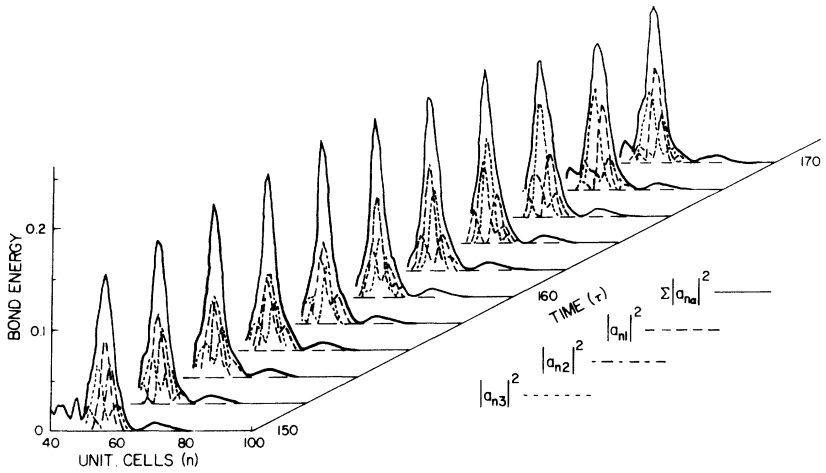

FIG. 6. Propagation on individual spines.

with a period $\mathscr{P}$, expressed in seconds, as

$$\mathscr{P} \doteq (0.54\times 10^{-12}) n_{\max} \ . \tag{3.9}$$

IV. ESTIMATION OF THRESHOLD AND INITIAL SOLITON SPEED

"What exactly *is* a soliton?" is a question often asked and up to now the dictionary does not provide an answer. To the purist a soliton is a solitary-wave solution for one of the several dozen systems that can be completely integrated via the inverse scattering transform (IST) method.[27] Applied scientists, however, often use the term for solitary-wave solutions of a dynamic system that is "close" to some completely integrable ideal. It is in this latter sense that the entities discussed here are called solitons, and a completely integrable ideal is the nonlinear Schrödinger NLS equation (2.9) displayed in Sec. II.

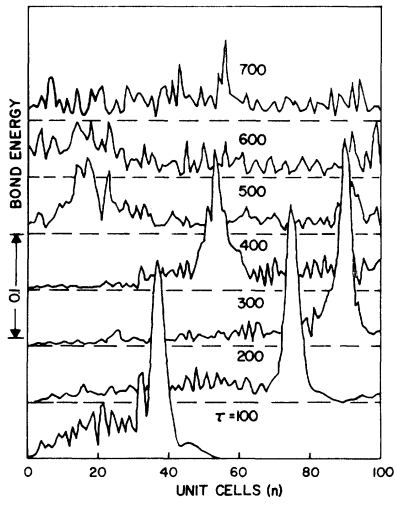

FIG. 7. Reflection of soliton from end.

To appreciate what we can learn about the solitary wave described in Sec. III from study of NLS, it is convenient to introduce the transformation

$$\phi \equiv \left[\frac{2(1-s^2)\bar{c}^6}{k_1 k_2 \chi^2}\right]^{1/2} \tilde{A} \ , \tag{4.1}$$

whereupon (2.9) takes the standard form

$$i\phi_\tau + \phi_{\xi\xi} = -2\,|\,\phi\,|^2\phi \ . \tag{4.2}$$

As $\phi(\xi,\tau)$ evolves according to (4.2), the eigenvalues λ of the associated linear problem

$$i\begin{bmatrix} \partial_\xi & -\phi \\ -\phi^* & -\partial_\xi \end{bmatrix}\cdot\begin{bmatrix}\psi_1 \\ \psi_2\end{bmatrix} = \lambda\begin{bmatrix}\psi_1 \\ \psi_2\end{bmatrix} \tag{4.3}$$

are independent of time.[22] Furthermore, the soliton solutions of (4.2) are uniquely related to the bound-state eigenfunctions of (4.3). For initial conditions

$$\phi = \begin{cases} \tilde{N}, & 0<\xi<p \\ -\tilde{N}, & -p<\xi<0 \\ 0, & |\,\xi\,|>p \end{cases} \tag{4.4}$$

which are a continuum approximation to (3.5), it was shown[10] that bound-state eigenvalues of (4.3) are upper half plane (UHP) roots in the λ plane of

$$mp\,\cot mp = i(\lambda p \pm \tilde{N}) \ , \tag{4.5}$$

where

$$m^2 \equiv \lambda^2 + \tilde{N}^2/p^2 \,. \tag{4.6}$$

Solitons appear in the solution to (4.2) as zeros of (4.5) move into the upper half plane: thus at the threshold for soliton formation, λ is real. This implies that the left hand side (lhs) of (4.5) is real while the right hand side (rhs) is pure imaginary, so the critical values of λ for soliton formation are

$$\lambda_j = \frac{\pi}{2\sqrt{2p}}(2j+1), \quad j=0,1,2,\ldots \tag{4.7}$$

and the corresponding soliton speeds are[23]

$$s_j = 4\lambda_j \,. \tag{4.8}$$

It was shown[10] that the speed of the first soliton, s_0, is very close to the peak velocity of a solution of the linear system $i\phi_\tau + \phi_{\xi\xi} = 0$ initialized by (4.4) which dominates below the threshold for soliton formation. The computations reported in Ref. 10 gave a value for s_0 about twice as large as that obtained from numerical study of the corresponding Davydov (*D*) system because (4.2) does not represent the dispersion associated with the discrete nature of *D*.

Figure 4 shows that for the MD system, the first soliton appears again with about the speed of the linear subthreshold response. But (4.7) predicts a "soliton window" in which the threshold for the second soliton is three times that for the first, while Fig. 3 shows this ratio to be less than 2:1. Also (4.7) indicates that the speed of the second soliton should be three times that of the first, while Fig. 4 shows it to be stationary, pinned near $n=0$.

In summary, then, the following points can be made concerning the usefulness of NLS for understanding the behavior of MD:

(1) NLS predicts a threshold for formation of a first soliton which is in order-of-magnitude agreement with that observed on MD.

(2) The speed of this first soliton is better calculated from analysis of the linear equation obtained by setting χ_1 and χ_2 equal to zero in (2.1a).

(3) NLS predicts multisoliton formation as is observed on MD, but the speed is completely wrong: $s_1 = 3s_0$ for NLS while $s_1 = 0$ on MD. Furthermore NLS fails to predict the eventual demise of the first soliton as is observed on Fig. 4.

V. PERTURBATION CALCULATIONS

In this section the Zakharov approximation to the MD equations are analyzed to obtain additional insight into the soliton dynamics. It is convenient to write (2.7) in the normalized form

$$iA_t + A_{xx} - \rho A = 0 \,, \tag{5.1a}$$

$$\rho_{tt} - \rho_{xx} - (|A|^2)_{xx} = 0 \,. \tag{5.1b}$$

A most useful discussion of the properties of Z' is given by Gibbons *et al.*[28] from which we read that conserved quantities are

$$P = \tfrac{1}{2}\int_{-\infty}^{\infty} [i(AA_x^* - A^*A_x) + 2\rho V]dx \,, \tag{5.2}$$

$$H = \int_{-\infty}^{\infty} (|A_x|^2 + \rho|A|^2 + \tfrac{1}{2}\rho^2 + \tfrac{1}{2}V^2)dx \,, \tag{5.3}$$

$$N = \int_{-\infty}^{\infty} |A|^2 dx \,, \tag{5.4}$$

where V is a "hydrodynamic flux" that is related to the sound variable by the conservation law

$$\rho_t + V_x = 0 \,. \tag{5.5}$$

(5.1) has a solitary wave solution

$$A(A_0,s) = A_0 \operatorname{sech}\frac{A_0(x-st)}{[2(1-s^2)]^{1/2}} \times \exp\left\{ i\left[\frac{sx}{2} - \left[\frac{s^2}{4} - \frac{A_0^2}{2(1-s^2)} \right] t \right] \right\}, \tag{5.6a}$$

$$\rho = -\frac{|A^2|}{1-s^2} \,. \tag{5.6b}$$

With the definition

$$m \equiv A_0[2(1-s^2)]^{1/2} \tag{5.7}$$

the solitary wave has conserved quantities[28]

$$N = 2m \,, \tag{5.8}$$

$$P = ms + \frac{2m^3 s}{3(1-s^2)^3} \,, \tag{5.9}$$

$$H = \tfrac{1}{2}ms^2 + \frac{s^3(5s^2-1)}{6(1-s^2)^3} \,. \tag{5.10}$$

Consider next the effect of applying initial conditions at $t=0$. It is convenient to note that if (5.1b) written as

$$\rho_{tt} - \rho_{xx} = \begin{cases} 0 \text{ for } t<0 \\ F(x,t) \text{ for } t>0 \end{cases}$$

then a solution is[29]

$$\rho(x,t) = \tfrac{1}{2}\int_0^t \int_{x-(t-t')}^{x+(t-t')} F(x',t')dx'\,dt' \,. \tag{5.11}$$

Now suppose that the sound system is driven by a solitary wave of the form $F(x,t) = G_{xx}(x-st)$; then

$$\rho = \frac{1}{1-s^2}G(x-st) - \frac{1}{2(1-s)}G(x-t)$$

$$-\frac{1}{2(1+s)}G(x+t)\,. \tag{5.12}$$

The response consists of a component locked to the solitary wave plus right and left traveling components at the sound speed. This behavior is also seen in the computations on MD shown in Fig. 3. Component B of the sound energy travels to the right at sound speed, while component A is locked to the soliton.

To this point no mention has been made of dissipative processes affecting the soliton. Two of these that must be considered are: (i) losses from the sound system, and (ii) losses from the bond-energy system. The approach taken here is to develop a perturbation theory that is inspired by, but not limited to, a true soliton-perturbation theory,[30] because the Zakharov system does not have an inverse scattering transform method and therefore is not, in the pure sense, a soliton system.

The analysis proceeds as follows. From Eqs. (5.7–5.10) it is clear that the speed (s) and the "mass" (m) of an isolated solitary wave [Eq. (5.6)] will remain constant on the unperturbed system (5.1). Adding a structural perturbation of order ϵ to (5.1) induces secular behavior in the first-order (order ϵ) correction to the solution. This secularity can be eliminated by choosing appropriate (order ϵ) expressions for the time derivatives $\dot{s}$ and $\dot{m}$, and it is just these time derivatives that determine the order ϵ dynamics of the solitary wave. The details of this approach are described in Appendix C, but the results are easily stated.

Energy loss from the sound system. To consider this effect, we augment (5.1) to

$$iA_t+A_{xx}-\rho A=0\,, \tag{5.13a}$$

$$\rho_{tt}-\rho_{xx}-(|A^2|)_{xx}=-\alpha\rho_t\,, \tag{5.13b}$$

and find (see Appendix C) that soliton speed and mass are modulated according to

$$P_s\dot{s}+P_m\dot{m}=-\tfrac{16}{3}\alpha m s\,, \tag{5.14a}$$

$$H_s\dot{s}+H_m m=-\tfrac{16}{3}\alpha m s^2\,, \tag{5.14b}$$

where expressions for $P(s,m)$ and $H(s,m)$ are given in (5.9) and (5.10). It is important to note that[28]

$$H_s=sP_s\,, \tag{5.15}$$

which, together with (5.14), implies

$$\dot{m}=0\,. \tag{5.16}$$

Thus either of (5.14) can be integrated to obtain

$$\ln\left[\frac{s^{1+2m^2/3}}{(1-s^2)^{1/2}}\right]=\frac{-16}{3}\alpha t+\text{const.} \tag{5.17}$$

For $s^2\ll 1$ (for solitons studied numerically in this paper $s^2=9/64$)

$$s\doteq s_0\exp\left[\frac{-16\alpha t}{3+2m^2}\right]\,, \tag{5.17'}$$

where s_0 is the soliton speed at time $t=0$.

It is shown in Appendix C that (5.16) holds for *any* perturbation of the sound system; it does not depend on the special form of dissipation chosen in (5.13b).

Energy loss from the bond system. In this case we augment (5.1) to

$$iA_t+A_{xx}-\rho A=i\beta A\,, \tag{5.18a}$$

$$\rho_{tt}-\rho_{xx}-(|A|^2)_{xx}=0\,, \tag{5.18b}$$

whereupon the modulation equations for s and m are

$$P_s\dot{s}+P_m\dot{m}=-2\beta m s\,, \tag{5.19a}$$

$$H_s\dot{s}+H_m\dot{m}=-\beta\left[ms^2-\frac{m^3}{(1-s^2)^2}\right]\,. \tag{5.19b}$$

The algebraic signs in (5.19b) can be appreciated if (5.19) is written in the form

$$\dot{P}=-2\beta P_{\text{ex}}\,, \tag{5.19a'}$$

$$\dot{H}=-2\beta(H_{\text{ex}}+H_{\text{int}})\,, \tag{5.19b}$$

where

$$P_{\text{ex}}=\tfrac{1}{2}\int_{-\infty}^{\infty}(AA_x^*-A_x^*A)dx\,, \tag{5.20a}$$

$$H_{\text{ex}}=\int_{-\infty}^{\infty}|A_x|^2dx\,, \tag{5.20b}$$

$$H_{\text{int}}=\int_{-\infty}^{\infty}\rho|A|^2dx\,. \tag{5.20c}$$

H_{int} is negative; that is what holds the solitary wave together.

In the special case $s=0$, (5.19) reduce to

$$\dot{m}=-2\beta m\,, \tag{5.20d}$$

which implies an exponential decay of bond energy with a time constant of $1/2\beta$. This is a reasonable assumption since, as Davydov, Eremko, and Sergienko have shown,[15] the decay time for bond energy in an isolated soliton is quite long.

Coupling between spines. As a further exercise with the perturbation theory, consider an approximation of the α helix in which a system like (5.1) is used to describe propagation on each of the three spines and coupling between spines is included as a

perturbation. Thus we consider the system

$$iA_{\alpha,t}+A_{\alpha xx}-\rho_\alpha A_\alpha=\epsilon(A_{\alpha+1}+A_{\alpha+2}) , \tag{5.21a}$$

$$\rho_{\alpha,tt}-\rho_{\alpha,tt}-(|A_\alpha|^2)_{xx}=0 , \tag{5.21b}$$

where $\alpha=1,2,3$ and the sums on α are "modulo three" (i.e., $2+2=1$, etc.). Calculating ϵ from the J (longitudinal coupling) and the L (transverse coupling) term Δ in (2.1) gives $\epsilon=0.033$. From the perturbation theory one obtains (to order ϵ)

$$\dot{P}_1+\dot{P}_2+\dot{P}_3=0 , \tag{5.22a}$$

$$\dot{H}_1+\dot{H}_2+\dot{H}_3=0 . \tag{5.22b}$$

Thus the soliton components on the three spines can be viewed as elastically interacting mass points. As previously noted from Fig. 6, the period of the corresponding oscillation is 2×10^{-12} sec.

Loss to additional mechanical modes. An important contribution to energy loss from the sound system will be stimulation of additional modes of vibration not included in the MD system that was studied numerically in Sec. III. Let us consider one of these modes which is described by the dynamic equation

$$y+\omega_0^2 y=\omega_0^2 y_0(t) , \tag{5.23}$$

where

$$\omega_0^2\equiv k/m_0 \tag{5.24}$$

and $k\,(m_0)$ are the effective spring constant (mass) of this mode. As a soliton passes by, the mode will be driven by a function of the form

$$y_0(t)=Y_0\,\mathrm{sech}^2(t/T)$$

and it is straightforward, though somewhat tedious, to calculate the increase in vibrational energy of the mode. It is

$$\Delta U=\frac{\pi^2}{8}kY_0^2F(\omega_0T) , \tag{5.25}$$

where

$$F(\omega_0T)=(\omega_0T)^4\left[\coth\left[\frac{\pi}{4}\omega_0T\right]-\tanh\left[\frac{\pi}{4}\omega_0T\right]\right] .$$

For $\omega_0T>1$, it is a very good approximation to write

$$\Delta U\doteq 2\pi^2kY_0^2(\omega_0T)^4\exp(-\pi\omega_0T) . \tag{5.25'}$$

Consider first the implications of these results for "optical" modes, i.e., those that take place within a unit cell of the α helix. The time duration of a soliton is $T=qd/s\bar{c}$, where q is the number of unit cells in a soliton, d is the length of a unit cell, and $s\bar{c}$ is soliton speed. Sound speed $\bar{c}=d\sqrt{w/M}$, thus

$$\omega_0T=\frac{q}{s}\left[\frac{M}{w}\frac{k}{m_0}\right]^{1/2} . \tag{5.26}$$

Since we expect $M>m_0$ and $w<k$,

$$\omega_0T>\frac{q}{s} . \tag{5.26'}$$

Furthermore $\frac{1}{2}kY_0^2$ will be less than the full soliton energy U, so

$$\frac{\Delta U}{U}<4\pi^2\left[\frac{q}{s}\right]^4\exp\left[-\pi\frac{q}{s}\right] . \tag{5.27}$$

Estimating roughly $q=5$ and $s=0.35$ given $\Delta U/U<10^{-14}$. Thus energy loss to optical modes will not be an important mechanism for energy dissipation.

Energy loss to "acoustic" modes (i.e., those that involve bending, twisting, or rotation of long sections of the α helix) could lead to $\omega_0T<1$ and therefore substantial energy loss as computed from (5.25). It is in just such situations that the soliton may be supposed to do useful work, but one should note from (5.16) that the "α" mechanism described here permits dissipation of only that portion of the total energy that is stored as kinetic sound energy. The arithmetic is as follows for total bond energy B and total sound energy S, expressed in joules:

$$B=NE_0$$

$$=3.28N\times10^{-20} , \tag{5.28}$$

$$S=\frac{1}{2}\left[M\left[\frac{d\beta_{n\alpha}}{dt}\right]^2+w(\beta_{n\alpha}-\beta_{n-1,\alpha})^2\right]$$

$$=\frac{w}{2}(\text{sound area})\times10^{-22} , \tag{5.29}$$

in joules where "sound area" is the cross-hatched region indicated in Fig. 3. Thus the percent of total energy that is carried as sound energy is

$$\frac{S}{B+S}\times100\doteq0.04\% . \tag{5.30}$$

In the dynamics described here, only the kinetic component of this sound energy will be dissipated as the soliton slows to a stop. Other mechanisms must be supposed to make use of the main portion of soliton energy.

It should be emphasized that the conclusions drawn from perturbation analysis of (5.1) hold only for an *isolated* solitary wave. The dissipation observed in Fig. 7 for $\tau > 270$ is probably caused by the interaction of the solitary wave with its tail. Further discussions of the propagation of solitons in a dissipative and noisy environment can be found in publications of Davydov and his coworkers.[31]

VI. CONCLUDING DISCUSSION

The primary aim of this research has been to decide whether it is reasonable to expect Davydov solitons to appear in real α-helix protein. Two factors contribute to this determination: the amount of energy to be transported by a soliton and the level of anharmonicity in a longitudinal hydrogen bond of α helix. Since ATP hydrolysis generates about 0.49 ev of free energy under normal physiological conditions, it is assumed that two (0.205 ev) amide-I quanta initialize an energy pulse. To compute the required level of hydrogen bond anharmonicity (χ_1) it was necessary to modify Davydov's original equations to include ten additional dipole-dipole coupling terms and to represent helical symmetry. With these changes soliton formation was observed for $\chi_1 > \chi_{1c} = 0.35 \times 10^{-10}$ N. This value is very close to the value $\chi_1 = 0.34 \times 10^{-10}$ N calculated independently for a similar hydrogen bond in the formamide dimer by Kuprievich and Kudritskaya.[12] Furthermore, dimensional arguments show that

$$\chi_{1c} \propto M^{-3/2},$$

where M is the mass of a unit cell of protein; so cross linkages, which can be expected to increase the effective value of M, should lower χ_{1c} to a value that is comfortably below 0.34×10^{-10} N. Thus the answer that emerges is: *Yes*, it is reasonable to expect Davydov solitons in real α-helix protein.

Having said this, several other questions arise. What functional roles can Davydov solitons be expected to play in living plants and animals? What special properties do they display? How might they be detected? To help answer such questions some numerical, analytical and perturbative calculations are included above from which the following results emerge.

(1) It should be possible to create Davydov solitons by direct stimulation with infrared radiation of 6.06 μm (corresponding to an amide-I absorption at 1650 cm^{-1}). This is clear because in the numerical study only bond energy was introduced as an initial condition.

(2) Davydov solitons should display a rather sharp internal resonance (related to exchange of energy between the three longitudinal spines of the α helix) with a period of about 2 psec or a free-space wavelength of about 600 μm.

(3) A piece of α helix with n unit cells (i.e., $3n$ peptide units) may show a broad resonance ("Q" $\doteq 1$) with a period of about $0.54n$ psec. Since the molecular weight (W_{mol}) of a strand of helix is about $114n$, this resonance should appear at a free-space wavelength of 1.42 $W_{mol} \times 10^{-4}$ cm. For this resonance to appear at a wavelength of 3 cm ("X-band" in RADAR jargon) the molecular weight would be about

$$W_{mol} = 21\,000 .$$

For the resonance to appear at 30 cm (1 GHz)

$$W_{mol} = 210\,000 .$$

(4) Mechanical effects induced directly by the soliton are limited to the kinetic part of the total energy. For the example studied here this is less than 0.02% (0.0002) of the total energy.

Several suggestions have been made concerning the functional roles that Davydov solitons may play or the ways they may appear in experimental biology. Some of these are the following.

(1) *Muscular contraction.* In 1979 Davydov[32] proposed that his solitons may be the key element in the contraction of striated muscle. His basic notion is that the longitudinal displacement of "thick" with respect to "thin" fibers is effected by a "lump" of solitons propagating more or less together toward the sarcomere center. As a variation on this theme, one might consider the model for contraction suggested recently by Jarosch.[33] This paper includes photographs of a mechanical model for muscular contraction in which torsional rotations of the thin filaments actually "screw" the fibers together. Although Jarosch provides structural arguments for the pitch of the screw, a soliton on one α helix of the coiled-coil structure might do as well. Following this line of thought, the coiled coil with one soliton might provide an explanation for a wide range of mechanical motions in living organisms.[27] It should be mentioned, however, that the model considered in this paper does not provide a mechanism for the transfer of amide-I bond energy from the soliton to

mechanical motion.

(2) *Sensitivity of living organisms to low-intensity nonionizing electromagnetic radiation.* Over the past decade a rather impressive amount of experimental evidence has been accumulating to indicate that living organisms are behaviorally sensitive to low-intensity e.m. radiation which raises tissue temperature only by "orders of magnitude less than 0.1 °C."[34] Proteinaceous material on cell membrane surfaces appears to be the site of detection, and it is clear that nonlinear mechanisms must be invoked to explain the extraordinary sensitivity observed. One such nonlinear mechanism is the influence of e.m. fields on the dynamics of Davydov solitons that play functional roles in vital processes of energy transport.[35,36]

(3) *Rupturing of α helix by tuberculosis and its effect on soliton dynamics.*[37] It has been suggested that the additional lines appearing in spectrofluorometric analysis of blood from tubercular patients is related to a change in the dynamics of Davydov solitons when α-helix protein molecules are ruptured by microbacterium tuberculosis.

(4) *Raman spectra shift in green algae.* Davydov solitons have recently been invoked to explain the temperature-dependent Raman spectrum of a green alga *(chlorella pyrenoidosa).*[38] In this picture the solitons are supposed to be excited by phase transitions that appear between 230 and 260 K and to spread the scattered energy over a larger number of vibrational modes.

(5) *The laser-Raman spectra of metabolically active cells.* After the foregoing manuscript was completely written, I became aware of the laser-Raman measurements on living cells recently published by Webb.[39] Among many other provocative facts, this report includes the following: (i) At 300 K a Raman spectrum is observed only when cells are metabolically active; (ii) the intensity ratios of Stokes to anti-Stokes lines indicate that the Raman active states are produced *in vivo* by nonthermal means; and (iii) spectral lines below 200 cm^{-1} shift to lower wave numbers as the cells progress through their life cycles. A particular spectrum of E. *coli* (taken from Fig. 7 of Ref. 39) shows, in Table II, the lines between 30 and 200 cm^{-1}.

Although broad laser-Raman spectra have been observed on α-helix proteins in aqueous solution and in crystalline form[40–42] and assigned to various linear modes of mechanical vibration, such an explanation is unlikely for the lines in Table II. As noted above, these lines appear *only* when an intact cell is metabolically active and move to lower wave numbers as the cell ages. Interpretation as the internal vibrational spectrum of Davydov solitons, however, is straightforward. One component of internal vibration is the "interspine oscillation" displayed in Fig. 6 which has a period of 2×10^{-12} sec, thus a spectral energy

$$E_1 = 17$$

in units of cm^{-1}. A second component is the "flutter" of the soliton as it moves past the unit cells of the lattice. Since the soliton speed is $\frac{3}{8}$ of the sound speed, (13) implies a period of $\frac{8}{3}\times10^{-13}$ sec or a spectral energy

$$E_2 = 125$$

in units of cm^{-1}. No "parameter adjustment" whatsoever has been involved in choosing these values for E_1 and E_2. The vibration spectrum of the soliton corresponds to these two energies and their sums and differences. Thus it is straightforward to construct Table III.

TABLE II. Laser-Raman lines measured from metabolically active E. coli.

Line no.	cm^{-1}
1	45
2	52
3	63
4	85
5	90
6	108
7	123
8	152
9	182

TABLE III. Laser-Raman lines calculated from modified Davydov equations.

Line no.	Structure	cm^{-1}
1	$2E_1$	34
2	$3E_1$	51
3	$4E_1$	68
4	$5E_1$	85
5	E_2-2E_1	91
6	E_2-E_1	108
7	E_2	125
8	E_2+2E_1	159
9	E_2+3E_1	176

Comparison between the measured lines in Table II and the calculated lines in Table III shows a striking similarity. Only line No. 1 is in substantial disagreeement and this may be in part due to measurement errors near the end of the run. Furthermore, the tendency of the measured lines to shift toward lower wave numbers as cells progress through their life cycles is gracefully explained by assuming that solitons receive less input energy and therefore move more slowly as a cell ages. Thus there is experimental evidence to suggest that Davydov solitons play a functional role in metabolic processes. See Ref. 43 for additional details.

ACKNOWLEDGMENTS

It is a pleasure to acknowledge many discussions with Prof. A. S. Davydov and with his associates, particularly V. Z. Enol'skii, A. A. Eremko, and A. I. Sergienko. Thanks are also due to V. A. Kuprievich and Z. G. Kudritskaja for providing an exact calculation of hydrogen bond anharmonicity, and to J. M. Hyman and L. MacNeil for help with the numerical code. The hospitality of the Institute of Theoretical Physics in Kiev (U. S. S. R.) and the Laboratory of Applied Mathematical Physics at Denmark's Technical University (where much of this work was done) is warmly appreciated.

APPENDIX A: STRUCTURE OF ADDITIONAL DIPOLE-DIPOLE COUPLING TERMS

Additional dipole-dipole coupling terms, indicated schematically in (2.11) are listed in this appendix. Relative locations of the dipole-dipole pairs can be understood with reference to Fig. 8. Here the two-digit index (01, 02, etc.) refers to an (n,α) designation for a particular amide-I bond. Letters $(L,N,J$, etc.) refer to a bond that is interacting with the bond located at $(n,\alpha)=(0,1)$ in the lower left-hand corner.

$$N:\ i\hbar\dot{a}_{n1}=-N(a_{n3}+a_{n-1,2})+\cdots\ ,$$
$$i\hbar\dot{a}_{n2}=-N(a_{n+1,1}+a_{n-1,3})+\cdots\ ,$$
$$i\hbar\dot{a}_{n3}=-N(a_{n+1,2}+a_{n1})+\cdots\ ;$$
$$P:\ i\hbar\dot{a}_{n1}=-P(a_{n+1,2}+a_{n-2,3})+\cdots\ ,$$
$$i\hbar\dot{a}_{n2}=-P(a_{n+1,3}+a_{n-1,1})+\cdots\ ,$$
$$i\hbar\dot{a}_{n3}=-P(a_{n+2,1}+a_{n-1,2})+\cdots\ ;$$

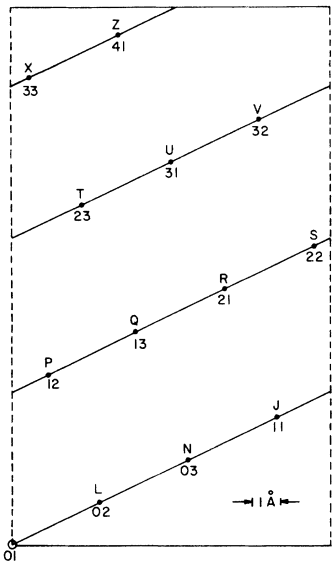

FIG. 8. Location of additional dipole-dipole coupling terms. (The reader can cut and join along the dashed lines to obtain a three-dimensional model of the helix.)

$$Q:\ i\hbar\dot{a}_{n1}=-Q(a_{n+1,3}+a_{n-2,2})+\cdots\ ,$$
$$i\hbar\dot{a}_{n2}=-Q(a_{n+2,1}+a_{n-2,3})+\cdots\ ,$$
$$i\hbar\dot{a}_{n3}=-Q(a_{n+2,2}+a_{n-1,1})+\cdots\ ;$$
$$R:\ i\hbar\dot{a}_{n1}=-R(a_{n+2,1}+a_{n-2,1})+\cdots\ ,$$
$$i\hbar\dot{a}_{n2}=-R(a_{n+2,2}+a_{n-2,2})+\cdots\ ,$$
$$i\hbar\dot{a}_{n}=-R(a_{n-2,3}+a_{n-2,3})+\cdots\ ;$$
$$S:\ i\hbar\dot{a}_{n1}=-S(a_{n+2,2}+a_{n-3,3})+\cdots\ ,$$
$$i\hbar\dot{a}_{n2}=-S(a_{n+2,3}+a_{n-2,1})+\cdots\ ,$$
$$i\hbar\dot{a}_{n3}=-S(a_{n+3,1}+a_{n-2,2})+\cdots\ ;$$
$$T:\ i\hbar\dot{a}_{n1}=-T(a_{n+2,3}+a_{n-3,2})+\cdots\ ,$$
$$i\hbar\dot{a}_{n2}=-T(a_{n+3,1}+a_{n-3,3})+\cdots\ ,$$
$$i\hbar\dot{a}_{n3}=-T(a_{n+3,2}+a_{n-2,1})+\cdots\ ;$$
$$U:\ i\hbar\dot{a}_{n1}=-U(a_{n+3,1}+a_{n-3,1})+\cdots\ ,$$
$$i\hbar\dot{a}_{n2}=-U(a_{n+3,2}+a_{n-3,2})+\cdots\ ,$$
$$i\hbar\dot{a}_{n3}=-U(a_{n+3,3}+a_{n-3,3})+\cdots\ ;$$
$$V:\ i\hbar\dot{a}_{n1}=-V(a_{n+3,2}+a_{n-4,3})+\cdots\ ,$$
$$i\hbar\dot{a}_{n2}=-V(a_{n+3,3}+a_{n-3,1})+\cdots\ ,$$
$$i\hbar\dot{a}_{n3}=-V(a_{n+4,1}+a_{n-3,2})+\cdots\ ;$$

$$X:\ i\hbar\dot{a}_{n1}=-X(a_{n+3,3}+a_{n-4,2})+\cdots\ ,$$
$$i\hbar\dot{a}_{n2}=-X(a_{n+4,1}+a_{n-4,3})+\cdots\ ,$$
$$i\hbar\dot{a}_{n3}=-X(a_{n+4,2}+a_{n-3,1})+\cdots\ ;$$
$$Z:\ i\hbar\dot{a}_{n1}=-Z(a_{n+4,1}+a_{n-4,1})+\cdots\ ,$$
$$i\hbar\dot{a}_{n2}=-Z(a_{n+4,2}+a_{n-4,2})+\cdots\ ,$$
$$i\hbar\dot{a}_{n3}=-Z(a_{n+4,3}+a_{n-4,3})+\cdots\ .$$

To appreciate the need for including this many additional coupling terms, consider Fig. 9 where comparisons can be made with the "standard" calculation of Fig. 9(a). In Fig. 9(c), Z has been set to zero and the difference with Fig. 9(a) is minor. In Fig. 9(d), both Z and $X=0$ and the soliton speed is slightly reduced. In Fig. 9(e), Z, X, and $V=0$, and the fraction of band energy going into the soliton is increased. This trend continues in Fig. 9(f) where Z, X, V, and $U=0$. Thus we observe a convergence toward the standard calculation of Fig. 9(a) as the terms: L-T [9(f)], L-U [9(f)] L-V [9(d)], and L-X [9(c)] are included in the calculation.

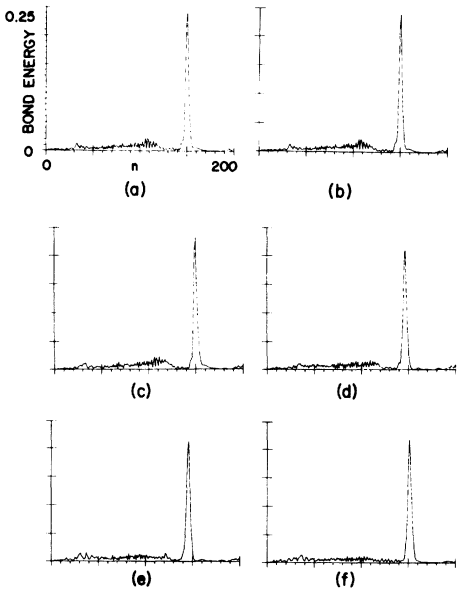

FIG. 9. Numerical comparisons. (a) standard calculation; (b) sound energy (W) included in (2.11); (c) Z coupling removed; (d) Z and X coupling removed; (e) Z, X, and V coupling removed; (f) Z, X, V, and U coupling removed.

APPENDIX B: STRUCTURE OF THE WAVE FUNCTION

In the development of Davydov, Eremko, and Sergienko,[15] the fundamental Hamiltonian

$$\hat{H}=\hat{H}_{\rm ex}+\hat{H}_{\rm ph}+\hat{H}_{\rm int}\ , \tag{B1}$$

where

$$\hat{H}_{\rm ph}=\tfrac{1}{2}\sum_{n\alpha}\left[\frac{1}{M}P_{n\alpha}^2+w(u_{n\alpha}-u_{n+1,\alpha})^2\right] \tag{B2}$$

and u and P are position and momentum operators for the helix satisfying

$$[u_{n\alpha},P_{n'\alpha'}]=i\hbar\delta_{nn'}\delta_{\alpha\alpha'}\ . \tag{B3}$$

They choose a wave function of the form

$$|\psi(t)\rangle=\sum_{n\alpha}a_{n\alpha}(t)e^{\sigma(t)}B_{n\alpha}^{\dagger}|0\rangle\ , \tag{B4}$$

where

$$\sigma(t)\equiv-\frac{i}{\hbar}\sum_{n\alpha}[\beta_{n\alpha}(t)P_{n\alpha}-\pi_{n\alpha}(t)u_{n\alpha}]\ . \tag{B5}$$

Thus

$$\langle\psi(t)|\hat{H}_{\rm ph}|\psi(t)\rangle=\sum_{n\alpha}a_{n\alpha}^{*}a_{n\alpha}W\ , \tag{B6}$$

where W is defined in Eq. (2.1c). Subject to the normalization constraint

$$\sum_{n\alpha}|A_{n\alpha}|^2=1\ , \tag{B7}$$

(B6) can be interpreted as the energy of the sound system. In order to remove the constraint (B7), it is convenient to define an approximate wave function with

$$\sigma(t)\equiv-\frac{i}{\hbar\sqrt{N}}\sum_{n\alpha}[\beta_{n\alpha}(t)P_{n\alpha}-\pi_{n\alpha}(t)u_{n\alpha}]\ , \tag{B8}$$

where

$$\sum_{n\alpha}|a_{n\alpha}|^2\equiv N,\ \text{and}\ |a_{n\alpha}|^2\le 1\ . \tag{B9}$$

Then

$$\langle\psi(t)|\hat{H}_{\rm ph}|\psi(t)\rangle=W \tag{B10}$$

and the total Hamiltonian in the ψ representation becomes

$$H=\sum_{n\alpha} a^*_{n\alpha}[E_0 a_{n\alpha}-J(a_{n-1,\alpha}+a_{n+1,\alpha})+L(a_{n,\alpha+1}+a_{n,\alpha-1})]$$
$$+\tfrac{1}{2}\sum_{n\alpha}\left[M\left[\frac{d\beta_{n\alpha}}{dt}\right]^2+w(\beta_{n\alpha}-\beta_{n-1,\alpha})^2\right]+\chi_1\sum_{n\alpha}[a^*_{n\alpha}a_{n\alpha}(\beta_{n+1,\alpha}-\beta_{n-1,\alpha})]$$
$$+\chi_2\sum_{n\alpha}[(\beta_{n\alpha}-\beta_{n-1,\alpha})(a^*_{n\alpha}a_{n-1,\alpha}+a^*_{n-1,\alpha}a_{n\alpha})]\ . \tag{B11}$$

With this modification, W does not appear in the first line of Eq. (2.1a).

Comparison of Fig. 9(a) and 9(b) shows that there is no change in the numerical result in the two cases: 9(a) W does not appear, and 9(b) W is included.

APPENDIX C: PERTURBATION ANALYSIS

Consider (5.13). It can be written as a fourth-order system involving only first-time derivatives. Thus

$$_tA-i\partial_{xx}A+i\rho A=0\ , \tag{C1a}$$
$$\partial A^*+i\partial_{xx}A^*-i\rho A^*=0\ , \tag{C1b}$$
$$\partial_t\rho-\sigma=0\ , \tag{C1c}$$
$$\partial_t\sigma-\partial_{xx}\rho-\partial_{xx}(AA^*)=-\alpha\sigma\ , \tag{C1d}$$

where $\sigma\equiv\rho_t$.

Expanding the solutions of (C1) in a power series in α

$$A=A_0+\alpha A_1+\cdots\ , \tag{C2a}$$
$$\rho=\rho_0+\alpha\rho_1+\cdots\ , \tag{C2b}$$
$$\sigma=\sigma_0+\alpha\sigma_1+\cdots\ , \tag{C2c}$$

we find that (A_0,ρ_0,σ_0) must satisfy (C1) with $\alpha=0$, and (A_1,ρ_1,σ_1) must satisfy the linear equations

$$\underbrace{\begin{bmatrix}(\partial_t-i\partial_{xx}+i\rho_0) & 0 & iA_0 & 0\\ 0 & (\partial_t+i\partial_{xx}-i\rho_0) & -iA_0^* & 0\\ 0 & 0 & \partial_t & -1\\ -\partial_{xx}A_0^* & -\partial_{xx}A_0 & -\partial_{xx} & \partial_t\end{bmatrix}}_{L}\times\begin{bmatrix}A_1\\ A_1^*\\ \rho_1\\ \sigma_1\end{bmatrix}=\begin{bmatrix}0\\ 0\\ 0\\ -\sigma_0\end{bmatrix}\ . \tag{C3}$$

The adjoint of the matrix L appearing on the lhs of (C3) is

$$L^\dagger=\begin{bmatrix}(-\partial_t+i\partial_{xx}-i\rho_0) & 0 & 0 & -A_0\partial_{xx}\\ 0 & (-\partial_t-i\partial_{xx}+i\rho_0) & 0 & -A_0^*\partial_{xx}\\ -iA_0^* & iA_0 & -\partial_t & -\partial_{xx}\\ 0 & 0 & -1 & -\partial_t\end{bmatrix}\ . \tag{C4}$$

This adjoint is defined with respect to the inner product

$$(v,u)\equiv\int_{-\infty}^{\infty}(v_1^*u_1+v_2^*u_2+v_3^*u_3+v_4^*u_4)dx\ . \tag{C5}$$

To avoid secular behavior (i.e., linear growth in time) of the order α corrections in (C2), it is necessary that the forcing function (i.e., rhs) of (C3) be orthogonal to $N(L^\dagger)$, the null space of $L^\dagger$. As (C3) is written, this is not possible. However, if the parameters s and m that appear in the zero-order solution are supposed to have an order α variation with time, then the rhs of (C3) becomes augmented to

$$\bar{F}=\frac{1}{\alpha}\begin{bmatrix} -A_{0,s}\dot{s}-A_{0,m}\dot{m} \\ -A^*_{0,s}\dot{s}-A^*_{0,m}\dot{m} \\ -\rho_{0,s}\dot{s}-\rho_{0,m}\dot{m} \\ -\sigma_{0,s}\dot{s}-\sigma_{0,m}\dot{m}-\alpha\sigma_0 \end{bmatrix}. \tag{C6}$$

The condition

$$\bar{F}\perp N(L^\dagger) \tag{C7}$$

defines first-order ode's for s and m.

To find the null space of $L^\dagger$ note that if col (v_1,v_2,v_3,v_4) lies in $N(L)$ then

$$\begin{bmatrix} v_1 \\ -v_2 \\ -i\partial_t \int\int (dx)^2 v_3 \\ +i\partial \int\int (dx)^2 v_3 \end{bmatrix}$$

lies in $N(L^\dagger)$. Two elements of $N(L)$ are

$$\bar{b}_1=\begin{bmatrix} A_{0,t} \\ A^*_{0,t} \\ \rho_{0,t} \\ \rho_{0,tt} \end{bmatrix},\quad \bar{b}_2=\begin{bmatrix} A_{0,x} \\ A^*_{0,x} \\ \rho_{0,x} \\ \rho_{0,xt} \end{bmatrix},$$

so corresponding elements of $N(L^\dagger)$ are

$$\bar{d}_1=\begin{bmatrix} A_{0,t} \\ -A^*_{0,t} \\ -i\int\int (dx)^2\rho_{0,tt} \\ -i\int\int (dx)^2\rho_{0,t} \end{bmatrix},\quad \bar{d}_2=\begin{bmatrix} A_{0,x} \\ -A^*_{0,x} \\ -i\int (dx)\rho_{0,t} \\ +i\int (dx)\rho_0 \end{bmatrix}.$$

The condition $(\bar{F},\bar{d}_1)=0$ implies, after integration by parts and rearrangement

$$H_s\dot{s}+H_m\dot{m}=-\alpha\int_{-\infty}^{\infty}\left[\int_{-\infty}^{x}dx'\rho_{0,t}\right]^2 dx \tag{C8a}$$

and the condition $(\bar{F},\bar{d}_2)=0$ implies

$$P_s\dot{s}+P_m\dot{m}=+\alpha\int_{-\infty}^{\infty}\left[\int_{-\infty}^{x}dx\,\rho_{0,t}\right]\times\left[\int_{-\infty}^{x}dx'\rho_{0,x'}\right]dx\,. \tag{C8b}$$

Equations (C8) appear in the text as (5.14).

If the structural perturbation introduced into the rhs of (C1d) were arbitrary, say $-\alpha f$, the rhs of (C8a) would be

$$-\alpha\int_{-\infty}^{\infty}\left[f\int_{-\infty}^{x}dx'\rho_{0,t}\right]dx$$

and that of (C8b) would be

$$+\alpha\int_{-\infty}^{\infty}f\left[\int_{-\infty}^{x}dx'\rho_{0,x'}\right]dx = -\frac{\alpha}{s}\int f\left[\int dx'\rho_{0,t}\right]dx\,,$$

so (5.15) still implies $\dot{m}=0$.

The other perturbation computations proceed in a similar way.

APPENDIX D: NUMERICAL DETAILS

Details of the numerical computations are identical to those described in Ref. 10.

[1]A. C. Scott, F. Y. F. Chu, and D. W. McLaughlin, Proc. IEEE 61, 1443 (1973).

[2]A. J. Hopfinger, *et al.* in *Solitons and Condensed Matter Physics,* edited by A. Bishop and T. Schneider (Springer, Berlin, 1978), p. 330; see also, N. C. Banik *et al.,* Phys. Rev. Lett. 43, 456 (1979).

[3]W. P. Su, J. R. Schrieffer, and A. J. Heeger, Phys. Rev. B 22, 2099 (1980); W. P. Su and J. R. Schrieffer, Proc. Natl. Acad. Sci. (U. S. A.) 77, 5626 (1980); and M. J. Rice and E. J. Mele, Solid State Commun. 35, 487 (1980).

[4]S. W. Englander *et al.,* Proc. Natl. Acad. Sci. (U. S. A.) 77, 7222 (1980).

[5]M. J. Rice *et al.,* Phys. Rev. Lett. 36, 432 (1976).

[6]See A. S. Davydov, Phys. Scr. 20, 387 (1979); and *Biology and Quantum Mechanics* (Pergamon, New York, 1982).

[7]F. L. Hock, *Energy Transformations in Mammals: Regulatory Mechanisms* (Saunders, Philadelphia, 1971), pp. 1–5.

[8]D. E. Green, Science 181, 583 (1973); Ann. N. Y. Acad. Sci. 227, 6 (1974).

[9]L. Pauling, *The Nature of the Chemical Bond* (Cornell University, Ithaca, 1960).
[10]J. M. Hyman, D. W. McLaughlin, and A. C. Scott, Physica D 3, 23 (1981).
[11]V. A. Kuprievich and V. E. Klymenko, Mol. Phys. 34, 1287 (1977).
[12]V. A. Kuprievich and Z. G. Kudritskaja, private communication.
[13]A. S. Davydov, Theor. Math. Phys. (USSR) 40, 831 (1980); A. S. Davydov and V. Z. Enol'skii, Zh. Eksp. Teor. Fiz. 79, 1887 (1980) [Sov. Phys.—JETP 52, 954 (1980)].
[14]H. Bilz *et al.*, Z. Naturforsch B 36, 208 (1981).
[15]A. S. Davydov, A. A. Eremko, and A. I. Sergienko, Ukr. Fiz. Zh. (Russ. Ed.) 23, 983 (1978).
[16]R. E. Dickerson and I. Geis, *The Structure and Action of Proteins* (Benjamin/Cummings, New York, 1969), p. 13.
[17]A. S. Davydov, *Theory of Molecular Excitons* (Plenum, New York, 1971), pp. 153–169.
[18]A. S. Davydov (private communication).
[19]N. A. Nevskaya and Yu N. Chirgadze, Biopolymers 15, 637 (1976).
[20]J. C. Eilbeck, "Davydov Solitons" a 16-mm mute film available from Swift Film Productions, 1 Wool Road, Wimbledon, London, SW20 0HN, England for £55.00.
[21]V. E. Zakharov, Zh. Eksp. Teor. Fiz. 62, 1745 (1972) [Sov. Phys.—JETP 35, 908 (1972)].
[22]V. E. Zakharov and A. B. Shabat, Zh. Eksp. Teor. Fiz. 61, 118 (1971) [Sov. Phys.—JETP 34, 62 (1972)].
[23]M. J. Ablowitz *et al.*, Stud. Appl. Math. 53, 249 (1974).
[24]G. R. Tristam and R. H. Smith, Adv. Protein Chem. 18, 227 (1963).
[25]Yu. N. Chirgadze and N. A. Nevskaya, Biopolymers 15, 607 (1976).
[26]S. Hatano, H. Ishikawa, and H. Sato, *Cell Motility: Molecules and Organization* (University Park, Baltimore, 1979).
[27]V. E. Zakharov, Physica D (in press).
[28]J. Gibbons *et al.*, J. Plasma Phys. 17, 153 (1977).
[29]C. C. Lin and L. A. Segel, *Mathematics Applied* (MacMillan, New York, 1974), p. 388. Note that the sign of this equation is incorrect.
[30]See, D. W. McLaughlin and A. C. Scott, Phys. Rev. A 18, 1652 (1978) and A. C. Scott, Phys. Scr. 20, 509 (1979) for expository applications of the method to the sine-Gordon equation. For an application to nerve equations, see, A. C. Scott and S. D. Luzader, Phys. Scr. 20, 395 (1979).
[31]A. S. Davydov, Zh. Eksp. Teor. Fiz. 78, 789 (1980) [Sov. Phys.—JETP 51, 397 (1980)]; A. S. Davydov and A. A. Eremko, Theor. Math. Phys. (USSR) 43, 367 (1980); L. S. Brizhik, Inst. Theor. Phys. (Kiev) (in press).
[32]A. S. Davydov, Int. J. Quantum Chem. 16, 5 (1979).
[33]R. Jarosch, in *Cell Motility: Molecules and Organization*, edited by S. Hatano, H. Ishikawa, and H. Sato (University Park, Baltimore, 1979), pp. 291–319.
[34]W. R. Adey, Proc. IEEE 68, 119 (1980); Physiol. Rev. 61, 435 (1981).
[35]L. S. Taylor, Science (in press).
[36]A. F. Lawrence and W. R. Adey, Neurological Res. (in press).
[37]M. M. Bajaj *et al.*, Bull. Am. Phys. Soc. 26, 51 (1981).
[38]E. Del Giudice, S. Doglia, and M. Milani, Phys. Scr. 23, 307 (1981).
[39]S. J. Webb, Phys. Rep. 60, 201 (1980).
[40]E. W. Small, B. Fanconi, and W. L. Peticolas, J. Chem. Phys. 52, 4369 (1970).
[41]K. G. Brown *et al.*, Proc. Natl. Acad. Sci. (U. S. A.) 69, 1467 (1972).
[42]L. Genzel *et al.*, Biopolymers 15, 219 (1976).
[43]A. C. Scott, Phys. Lett. 86A, 60 (1981); Phys. Scr. (in press).